

Tracing non-equilibrium plasma dynamics on the attosecond timescale in small clusters

Ulf Saalman, Ionuț Georgescu and Jan M. Rost

Max Planck Institute for the Physics of Complex Systems
Nöthnitzer Straße 38, 01187 Dresden, Germany

E-mail: us@pks.mpg.de

Abstract. It is shown that the energy absorption of a rare-gas cluster from a vacuum-ultraviolet (VUV) pulse can be traced with time-delayed extreme-ultraviolet (XUV) attosecond probe pulses by measuring the kinetic energy of the electrons detached by the probe pulse. By means of this scheme we demonstrate, that for pump pulses as short as one femtosecond, the charging of the cluster proceeds during the formation of an electronic nano-plasma inside the cluster. Using moderate harmonics for the VUV and high harmonics for the XUV pulse from the same near-infrared laser source, this scheme with well defined time delays between pump and probe pulses should be experimentally realizable. Going to even shorter pulse durations we predict that pump and probe pulses of about 250 attoseconds can induce and monitor non-equilibrium dynamics of the nano-plasma.

PACS numbers: 31.70.Hq, 82.33.Fg, 05.70.Ln, 52.27.Gr

1. Introduction

The development of ultrashort attosecond laser pulses is taking breathtaking development. With isolated pulses already technically possible [1] attosecond pulses or pulse trains are presently used in combination with a strong near-infrared (NIR) pulse from which the attosecond pulses were generated in the first place. Although the strong NIR pulse modifies in many cases the target, it conveniently provides a clock which indicates at which time t the atto pulse acted on an electron, since the final momentum $\vec{p}_{\text{final}} = \vec{p}_{\text{excited}} + e\vec{A}(t)$ of an ionized electron contains as drift momentum the vector potential $\vec{A}(t)$ of the NIR field at time t and is therefore streaked by the NIR pulse [2, 3].

We have proposed a different pump-probe scheme: A VUV pulse (about 100 fs duration and 20 eV frequency) excites a rare-gas cluster, and the evolution of the electron dynamics is traced by a time-delayed attosecond pulse. While such a combination promises to deliver insight into fast dissipative multi-electron dynamics in the cluster [4], it is still experimentally out of reach. However, one can generate the VUV pulse from harmonics of a strong NIR pulse and combine it with an atto pulse. The prize to pay is that the VUV pulse will be relatively short, namely a few femtoseconds which is almost a factor 100 shorter than before [4]. Here, we explore this new scenario which, moreover, gives rise to new phenomena in the cluster dynamics as will be detailed below.

After introducing our approach in Sect. 2, we analyze in Sect. 3 the dynamics of small argon clusters with 13 and 55 atoms under a VUV pulse of a few femtoseconds and an attosecond probe pulse, focusing on mapping out the charging of the cluster which happens dominantly during the rising part of the VUV pulse. This scenario extrapolates the one studied before [4] to shorter excitation times. We find an interesting new phenomenon in a small time window at the crossover between instant and delayed ionization. To understand this phenomenon we replace the pump pulse in Sect. 4 with a sudden excitation of electrons. It turns out that their subsequent dynamics is that of a strongly-coupled non-equilibrium plasma [5] which oscillates between kinetic and potential energy with the plasma frequency, indeed explaining the crossover found in Sect. 3 as the reminder of this non-equilibrium dynamics when excited and probed with relatively long pulses. Consequently, we demonstrate in Sect. 5 that one can indeed observe this non-equilibrium plasma dynamics if attosecond pump and probe pulses are used, by tracing the potential energy in form of the charging of the cluster, as described before. We summarize our results in Sect. 6.

2. Theoretical method

In order to simulate the dynamics of electrons and cluster ions upon excitation by VUV laser pulses we have used a hybrid approach which combines quantum-mechanical absorption rates for bound electrons and classical propagation of the photo-ionized electrons. The approach is similar to those successfully applied to cluster dynamics

driven by NIR laser pulses [6]. Details of the adaption to the VUV regime have been published elsewhere [7]. Therefore we will only briefly review the main steps and assumptions here. Bound electrons may absorb photons according to known photo-absorption rates [8], i. e., there is a certain probability for absorption within a given time step. Due to this statistical feature one has to average over an ensemble of realizations, where each realization is a deterministic ionization sequence and the ensemble, containing typically about 100 realizations, is in accordance with the absorption rate. After their “creation” the electrons are propagated classically in the field of the laser and all previously generated electrons and ions. In contrast to photo-absorption of isolated atoms, electrons are not necessarily free but may be trapped in the cluster potential, i. e., by the attractive Coulomb potential of neighbouring ions. These electrons are called quasi-free electrons. Whereas the classical propagation is straight forward, it is challenging to properly describe the impact of the electrons and ions on further ionization of bound electrons. We have developed a method for calculating the photo-ionization rates in clusters which takes into account localization of electrons around a particular ion [7]. This “classical recombination” is of minor importance for the short pulses studied here but becomes relevant for longer pulses [4] as produced by free-electron-laser sources.

3. Observation of transient cluster charging

We will study the transient charging of small clusters using a pump-probe scenario proposed recently [4]. The clusters are excited by a VUV pump pulse which lasts—in contrast to our previous study—only for a few femtoseconds and probed with time-delayed attosecond XUV pulses. The instantaneous charge at time t is imprinted in the final kinetic energy of the electron released during the attosecond pulse which is shifted with respect to the peak of the pump pulse by a time delay t . Slower electrons indicate higher charges. In order to obtain absolute values we compare the energy reduction to the series of ionization potentials of the subsequent charge states of argon. The parameters chosen for the pump and probe pulses are motivated by their experimental availability [9]. Both pulses are most easily obtained from filtering of (different) harmonics from a driving NIR laser. Besides a flexible duration of the pump pulse, most importantly, this enables an accurate setting of the delay of the probing XUV pulse. The intensity of the probe pulse is of minor importance. On average less than one electron is photo-ionized per pulse due to the low cross sections for XUV frequencies. A lower intensity can be compensated by a higher repetition rate.

Figure 1 and 2 show the charging for Ar_{13} and Ar_{55} clusters, respectively. In both cases the pump frequency was $\hbar\omega = 20$ eV. For the smaller cluster we kept the intensity I constant and changed the pulse duration τ ; for the larger cluster we did it *vice versa*. Photo-absorption due to the pump pulses leads to excitation of electrons either directly into the continuum or—due to the increasing space charge—into the cluster. In either of the cases the electron is lost from the mother ion and the ionic charge increases. These

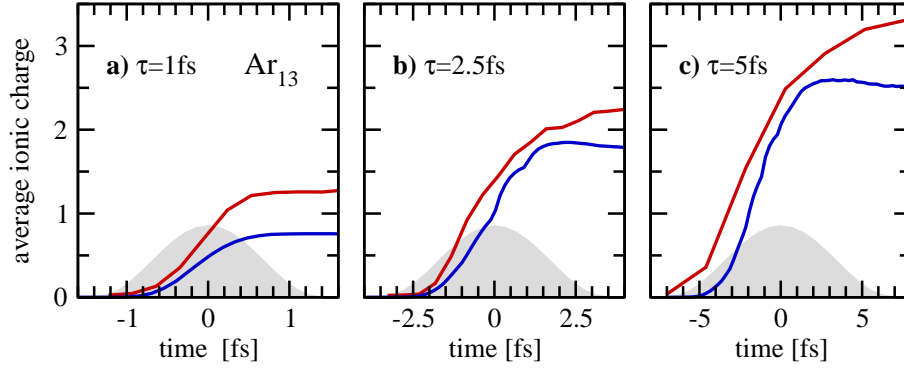


Figure 1. Average charge of ions in an Ar_{13} induced by laser pulses (gray shaded areas) with three different pulse lengths $\tau = 1$ fs, 2.5 fs, and 5 fs and the central frequency $\hbar\omega = 20$ eV and the same intensity $I = 7 \times 10^{13}$ W/cm². We compare the ionic charge (blue lines) due to photo-ionization of the pump pulse with the charge probed by the kinetic of the delayed attosecond pulse (red lines), see text for details.

charges, averaged over all cluster ions, are shown by the blue lines in Figs. 1 and 2. The maximum of the ionization rates (strongest increase) shifts to earlier times if the pulse is made longer (as from Figs. 1a to c) or if the intensity is increased (as from Figs. 2a to b). This is due to the depletion of the atoms in the cluster. It becomes relevant for average ionic charges larger than one, which is the case in Figs. 1b, c, and 2b. For the “long” pulse with $\tau = 5$ fs one observes localization or recombination of electrons which results in a decreased charge at the falling edge of the pulse, i. e., for times $t > 2.5$ fs. During the pulse we do not find noticeable localization.

The ionic charge as obtained from the attosecond probe pulses ($\hbar\omega = 150$ eV, $I = 10^{15}$ W/cm², $\tau = 500$ as) is shown by red lines in the Figs. 1 and 2. In this case the horizontal axis corresponds to the time delay of the probe pulses. Although the probing does not resemble the charging process perfectly for all cases, it performs particularly well when the charging is strongest, namely slightly before the pulse maximum. There

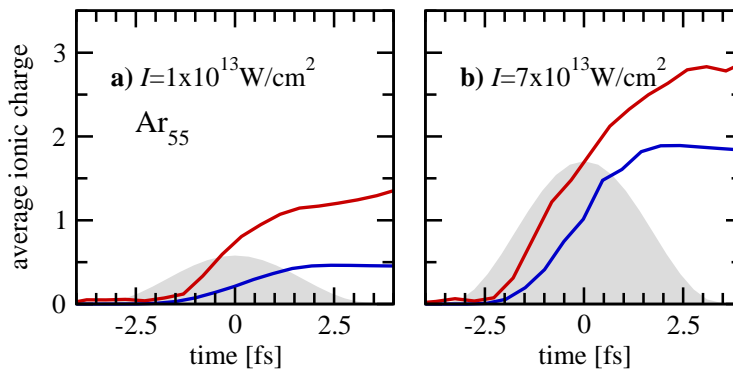


Figure 2. Same quantities as in Fig. 1, but for an Ar_{55} cluster and laser pulses of the same duration $\tau = 2.5$ fs and but two different intensities $I = 1 \times 10^{13}$ W/cm² and 7×10^{13} W/cm².

are basically three reasons for the apparent deviations: i) The space charge reduces the kinetic energy of the probing electrons and results in an overestimation of the ion charges. This effect is more important for Ar₅₅ as compared to Ar₁₃ because of the larger cluster charge. ii) Evaporation of quasi-free electrons increases the space charge as well. This effect becomes relevant only late in time, in our examples, after the pump pulse is over, see the deviation of both quantities in Fig. 1c. iii) For either very short (Fig. 1a) or very weak (Fig. 2a) pulses both quantities show an (almost linearly) increasing divergence already at early times. Note the difference to the other cases, where both curves are largely parallel during the initial charging. The increasing divergence is due to the low number of electrons captured by the cluster potential. Since the cluster does not host a plasma which would allow for screening of the ionic charges, the increasing space charge is directly imprinted in the probing signal.

Since the total cluster charge influences the probing signal, it is presented in Fig. 3 as a function of time for the cases considered above. It is defined by the number of electrons with positive energy $E > 0$. The energy of the j th electron (mass m , charge $-e$) with velocity \vec{v}_j is given by

$$E_j = \frac{m\vec{v}_j^2}{2} - \sum_{i(\neq j)}^{\text{all}} \frac{q_i e^2}{|\vec{r}_i - \vec{r}_j|}, \quad (1)$$

whereby the sum runs over all (except the electrons itself) charged particles with charge $q_i e$ at the position \vec{r}_i . In order to make Ar₁₃ and Ar₅₅ comparable the cluster charge is normalized to the number of cluster atoms. In all cases the charging of the cluster shows clearly two phases, namely fast direct charging early in the pulse and slow evaporation towards the end of the pulse and later on. Whereas for the longer pulses and Ar₁₃, cf. green and blue lines in Fig. 3a, these phases are separated by a plateau, in the other cases the cluster charge even drops after a maximum before evaporation sets in. Comparison with Figs. 1 and 2 reveals that this “overshooting” is connected with a

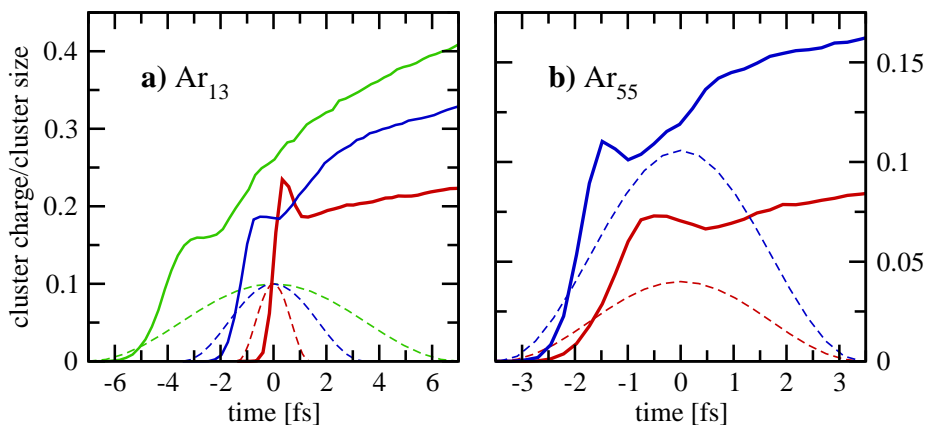


Figure 3. Total charge of the cluster, i. e., number of electrons with positive energy, divided by the cluster size. Left panel: cluster and laser pulse parameters as in Fig. 1, right panel: as in Fig. 2. The envelopes of the electric fields for the corresponding pump pulses are shown by dashed lines.

high photo-absorption rate, i. e., a large number of atoms becomes ionized within short time interval. This is either due to a quick rising[‡] of the laser intensity, as for the 1-fs-pulse, or due a large number of available atoms, as for Ar₅₅. The plateau or even the overshooting of the charge at the crossover from direct ionization to evaporation is most easily understood if one considers the limit of instant ionization of the electrons.

4. Instantaneous cluster ionization: Formation, equilibration and relaxation of a nano-plasma

Modelling instant ionization we assume for simplicity that all electrons absorb simultaneously one photon. Figure 4 shows the results for an Ar₅₅ cluster where one electron per atom was released at time $t = 0$ with an excess energy $E_0 = 4.24$ eV, according to a photon frequency $\hbar\omega = 20$ eV and the ionization potential of neutral argon $E_{\text{IP}} = 15.76$ eV; from that time on they are propagated classically. At the time of creation all electrons have positive energy and the cluster charge is equal to the cluster size as seen in Fig. 4a. This corresponds to the temporary enhancements seen in Fig. 3 and discussed before. The value drops down to about 0.2 similar to the values observed in the realistic calculations for Ar₁₃ and Ar₅₅. This drop is easily understood considering that the Coulomb energy of 55 singly-charged ions is larger than 3 keV. The total excess energy of the 55 electrons is, however, only about 233 eV. Thus for energetic reasons the majority of the electrons cannot leave the cluster volume.

More insight regarding the electron dynamics is gained by taking a closer look on the electron energies. Figure 4b shows separately the potential and kinetic energy of all quasi-free electrons. Their sum is approximately constant, violated only slightly through electrons which leave the cluster. This violation is small because, firstly, the number of electrons which leave the cluster during this time is negligible and, secondly, those which are lost carry only a very small amount of energy. Apparently there is an oscillatory exchange of potential and kinetic energy. The period of this oscillation is $\tau_{\text{osc}} \approx 0.79$ fs, which agrees with plasma period $\tau_{\text{pl}} = 2\pi/\omega_{\text{pl}} = \sqrt{\pi m/\rho e^2} = 0.77$ fs according to the atomic density ρ of argon at equilibrium structure[§]. Obviously those electrons which could not leave the cluster execute plasma oscillations.

That a plasma has formed on this short time scale may be surprising but can be seen in Fig. 4c. For selected times, shown by dots in Fig. 4c, we have calculated the velocity distribution of the quasi-free electrons. This distribution is fitted well for all times by the following function [10]

$$f_{v_0, \Delta v}(v) = C \cdot v^2 \cdot \exp\left(-\frac{(v-v_0)^2}{\Delta v^2}\right) \quad (2)$$

with C an irrelevant normalization constant. The distribution of Eq. (2) contains both

[‡] The ionization rate in panel a of Fig. 1 is considerably larger than in panel c, which is somehow hidden by the different time scales.

[§] The density is calculated for 55 atoms and a cluster radius of 8.5 Å. Atomic motion due to Coulomb explosion can be neglected on the considered time scale of a few femtoseconds.

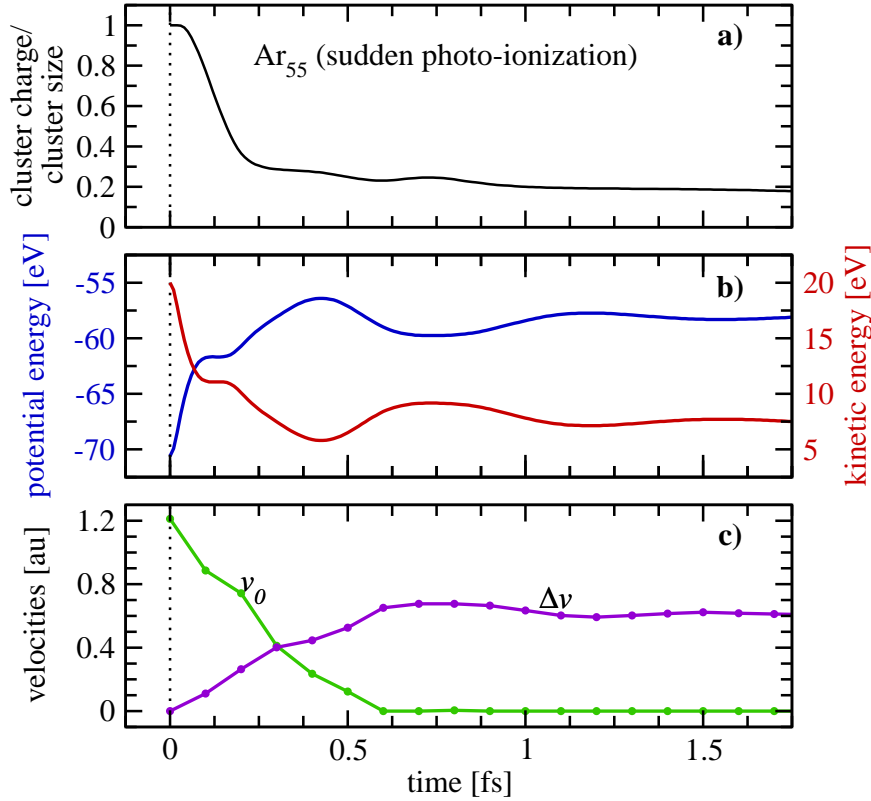


Figure 4. Time evolution after sudden single-photo-ionization of all atoms of an Ar_{55} cluster. From top to bottom: **a)** total charge of the cluster divided by the cluster size, **b)** potential (blue, right axis) and kinetic (red, left axis) energy of quasi-free electrons, i. e. electrons with negative energy, **c)** fit parameter for the velocity distribution of Eq. (2).

limits: monoenergetic electrons (with energy E_0) which corresponds to $v_0 = \sqrt{2E_0/m}$ and $\Delta v \rightarrow 0$ and an electron plasma at equilibrium (with temperature T) which corresponds to $v_0 = 0$ and $\Delta v = \sqrt{2kT/m}$. Hence, the ratio $v_0/\Delta v$ characterizes the degree of relaxation to equilibrium as a function of time. Starting with an infinitely large value at time $t = 0$ fs the ratio vanishes around $t = 0.6$ fs. Thus, the relaxation of the electronic distribution function takes about $\tau_{\text{rel}} = 0.6$ fs which is of the same order as the built-up of electronic correlations characterized by the plasma period $\tau_{\text{corr}} = 0.77$ fs. It is known from one component plasmas [11] as well as from ultracold plasmas [12] that in this situation the plasma temperature undergoes oscillations about its equilibrium value if the plasma is strongly coupled, i. e., if the Coulomb-coupling parameter

$$\Gamma = \frac{E_{\text{pot}}}{E_{\text{kin}}} > 1, \quad (3)$$

with E_{pot} and E_{kin} the potential and kinetic energy of the quasi-free electrons, respectively. For the system studied here we find $\Gamma \approx 6$. The oscillations are damped out quickly in about two plasma periods which is typical for an inhomogeneous plasma [5]. Discussing kinetic and potential energy of the electrons as a function of time assumes that we have an ideal “probe” of infinite time-resolution to record these energies. In the

next section we discuss how close one can come to this ideal with attosecond pulses.

5. Creating and monitoring of non-equilibrium plasmas in clusters with attosecond pump-probe pulses

With today's attosecond technology it is possible to come very close to the sudden excitation assumed in the previous section. If both, the pump *and* the probe pulse, have sub-femtosecond length, the non-equilibrium plasma oscillations can be observed by monitoring the time-dependent charging of the cluster as described in Sect. 3. We have chosen $\tau = 250$ as in order to ensure that the creation and probing of the plasma is fast on its time scale given by the plasma period of 770 as (see previous section). Otherwise the scenario is equivalent^{||} to that in Sect. 3. We measure the kinetic energy of electrons kicked out by the probe pulse ($\hbar\omega = 150$ eV) as a function of the time delay. Thereby, we obtain the time-dependent charge which is close to the charge of the cluster if the pump pulse is short as discussed in Sect. 3.

Figure 5 shows the probed charge (blue solid lines) for two pump laser frequencies $\hbar\omega = 20$ eV and 30 eV. Evidence for plasma oscillations are given by the calculated kinetic energy of the electrons (red solid lines). Oscillations become apparent after the initial energy drop during which the plasma formation occurs. They are more pronounced for the lower pump frequency (Fig. 5a) where on average one electron per atom is photo-ionized (blue dashed line). In the other case (Fig. 5b), with a lower electron density and longer plasma period, only one oscillation is visible. Similar to this

^{||} In contrast to the femtosecond pulses of Sect. 3 one has to consider the large bandwidth of the attosecond pulse, which is taken into account by initiating the classical electron motion after photo-absorption with the corresponding energy spread.

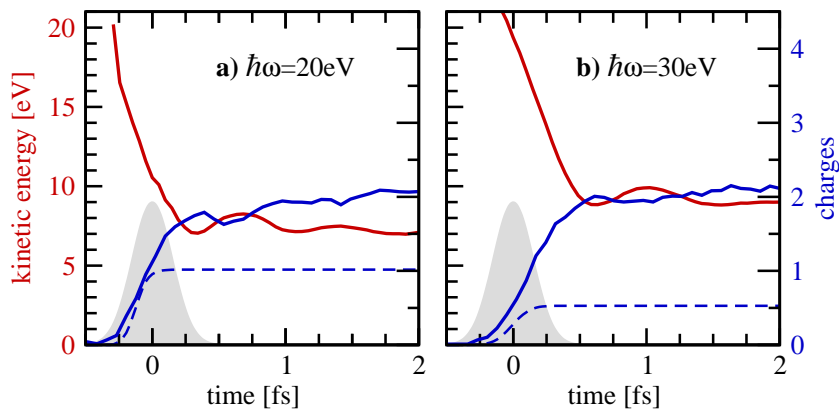


Figure 5. Time evolution after pumping of an Ar_{55} cluster by an attosecond VUV pulse (gray shaded areas) with duration $\tau = 250$ as, intensity $I = 5 \times 10^{14}$ W/cm² and **a)** $\hbar\omega = 20$ eV or **b)** $\hbar\omega = 30$ eV, respectively. The average kinetic energy (red lines, left axis) is shown along with the probed charge (solid blue lines, right axis). For completeness we show the ionic charges (dashed blue lines, right axis) which stay constant after the pulse.

theoretical quantity one observes a stronger contrast in the *measurable* probed charge for $\hbar\omega = 20\text{ eV}$ than for $\hbar\omega = 30\text{ eV}$. These oscillations are solely due to oscillating charge distribution; the ionic charges (blue dashed lines) remain constant after the pulse is over.

Although the attosecond pulse generated nano-plasma in the cluster differs by orders of magnitude in density, temperature and absolute number particles from an ultracold “micro”-plasma [13], we find very similar behavior for both finite plasmas, namely a fast decay of the plasma oscillations and more pronounced plasma oscillations for a larger Coulomb-coupling parameter Γ . In our case this is realized for 20 eV excitation frequency as compared to 30 eV, where for the former the density is higher (cf. blue dashed lines in Fig. 5) and the temperature is lower (cf. red lines in Fig. 5), hence the plasma is more strongly coupled. These observations are in accordance with the predictions from extended plasmas [11].

6. Summary

We have demonstrated that an attosecond pump-probe scheme opens the way to study non-equilibrium plasma phenomena in nano-plasmas created from finite systems such as rare-gas clusters. Initiated by a VUV pump pulse, the XUV probe pulse can map out energy absorption of the finite multi-electron system — represented in our case by a small rare-gas cluster — *during* the creation of the electronic nano-plasma. Alternatively, the probe pulse can be used to trace the non-equilibrium dynamics of the plasma including its relaxation *after* its creation. In both cases, ultrafast photo-ionization of the cluster ions triggered by the probe pulse is used to determine the charging of the cluster which provides directly the information on energy absorption in the first case and on plasma oscillations indicative of non-equilibrium dynamics in the second case.

The fast time scale for the formation of correlation as well as the plasma oscillations indicate the formation of a strongly-coupled plasma which has been built up due to the high density of the cluster ions in combination with the relatively low energy of the electrons [14]. Hence, the scheme proposed offers a route to make strongly-coupled plasmas in clusters experimentally accessible, which would boost our knowledge on dynamics in finite correlated multi-electron systems. These aspects will be investigated in more detail in future work [15].

References

- [1] Sansone G, Benedetti E, Calegari F, Vozzi C, Avaldi L, Flammini R, Poletto L, Villoresi P, Altucci C, Velotta R, Stagira S, De Silvestri S and Nisoli M 2006 *Science* **314**, 443.
- [2] Drescher M, Hentschel M, Kienberger R, Uiberacker M, Yakovlev V, Scrinzi A, Westerwalbesloh T, Kleineberg U, Heinzmann U and Krausz F 2002 *Nature* **419**, 803.
- [3] Kienberger R, Goulielmakis E, Uiberacker M, Baltuska A, Yakovlev V, Bammer F, Scrinzi A, Westerwalbesloh T, Kleineberg U, Heinzmann U, Drescher M and Krausz F 2004 *Nature* **427**, 817.
- [4] Georgescu I, Saalman U and Rost J M 2007 *Phys. Rev. Lett.* in press.
Preprint at <http://arxiv.org/abs/0705.3389>.
- [5] Pohl T, Pattard T and Rost J M 2005 *Phys. Rev. Lett.* **94**, 205003.
- [6] Saalman U, Siedschlag C and Rost J M 2006 *J. Phys. B* **39**, R39.
- [7] Georgescu I, Saalman U and Rost J M 2007 *Phys. Rev. A* in press.
Preprint at <http://arxiv.org/abs/0705.3387>.
- [8] Cowan R D 1981 *The Theory of Atomic Structure and Spectra* University of California Press Berkeley and CA.
- [9] Krausz F 2007, private communication.
- [10] MacDonald W M, Rosenbluth M N and Chuck W 1957 *Phys. Rev.* **107**, 350.
- [11] Zwicknagel G 1999 *Contrib. Plasma Phys.* **39**, 155.
- [12] Killian T C, Lim M J, Kulin S, Dumke R, Bergeson S D and Rolston S L 2001 *Phys. Rev. Lett.* **86**, 3759.
- [13] Killian T C, Pattard T, Pohl T and Rost J M 2007 *Phys. Rep.* **449**, 77.
- [14] Ramunno L, Jungreuthmayer C, Reinholz H and Brabec T 2006 *J. Phys. B* **39**, 4923.
- [15] Georgescu I, Saalman U and Rost J M 2007, in preparation.